HBRC Journal (2015) xxx, xxx–xxx

Housing and Building National Research Center

HBRC Journal

http://ees.elsevier.com/hbrcj

The effect of replacing sand by iron slag on physical, mechanical and radiological properties of cement mortar

Ahmed S. Ouda [a,*], Hamdy A. Abdel-Gawwad [b]

[a] Tabuk University, Taymaa Branch, Saudi Arabia
[b] Housing and Building National Research Center, Egypt

Received 14 December 2014; revised 1 April 2015; accepted 22 June 2015

KEYWORDS

Basic-oxygen furnace slag;
Cement mortars;
Fine aggregate;
Linear attenuation coefficient;
Half value layer;
Tenth value layer

Abstract In the present study, the effects of replacing sand by high percentages of basic-oxygen furnace slag on the compressive strength, bulk density and gamma ray radiation shielding properties of mortar have been investigated. Cement mortar of mix proportion 1:3 including various percentages of iron slag was designed. The percentages of replacement were 0%, 40%, 80% and 100% by weight of fine aggregate. Mortar mixes were prepared with water cement ratio of 0.44 and cured in potable water for 90 days. The attenuation measurements were performed using gamma spectrometer of NaI (Tl) detector. The utilized radiation sources comprised ^{137}Cs and ^{60}Co radioactive elements with photon energies of 0.662 MeV for ^{137}Cs and two energy levels of 1.17 and 1.33 MeV for the ^{60}Co. Likewise, half value layer (HVL), tenth value layer (TVL) and the mean free path (mfp) for the tested samples were measured. Results of this investigation indicated that the strength properties of mortars increased significantly upon replacing sand partially by iron slag. It was also observed that the inclusion of iron slag as partial replacement with fine aggregate enhances the bulk density of mortar. On the other hand, full sand replacement by iron slag has significant effects on shielding efficiency in thick shields, as it reduces the capture gamma rays better than normal mortar incorporating sand.

Introduction

Recycling or reuse of industrial by-products and wastes is economically and/or ecologically very important. The aggregates typically account for 70–80% of the concrete volume and play a substantial role in different concrete properties such as workability, strength, dimensional stability and durability. The use of different waste materials shows prospective application in construction industry as an alternative to conventional

* Corresponding author.
E-mail address: Ahmed.Kamel56@yahoo.com (A.S. Ouda).

Peer review under responsibility of Housing and Building National Research Center.

ELSEVIER Production and hosting by Elsevier

http://dx.doi.org/10.1016/j.hbrcj.2015.06.005

materials. Such practice conserves natural resources and reduces the space required for the landfill disposal of these waste materials. The aggregates used for mortar and concrete can be conveniently divided into dense and lightweight aggregates. The former class includes all the aggregates normally used in mass and reinforced concrete such as sand, gravel, crushed rocks and iron slag. Steel slag is a material which could be used as a partial replacement for fine aggregate [1]. The consumption of waste materials can be increased manifold if they are used as aggregates in both cement mortar and concrete. These types of uses of waste materials can solve problems of lack of aggregates in various construction sites and reduce environmental problems related to aggregate mining and waste disposal. The use of waste aggregates can also reduce the cost of concrete production. Due to the fact that aggregates can significantly affect the properties of concrete, consequently, a thorough evaluation is necessary before using any waste material as aggregate in concrete. A range of slag textures could be formed by differing the cooling regimes and the resultant slag types exhibit different properties. Blast furnace slag is a nonmetallic material consisting of silicates and aluminosilicates of calcium and magnesium together with other compounds of sulfur, iron, manganese and other trace elements. Air-cooled slag, which is allowed to solidify slowly in ladles or pits, is by far the most abundant and is a rock-like material which is almost wholly crystalline [2]. Blast-furnace slag aggregates generally have desirable properties such as soundness, strength, shape, abrasion resistance and gradation. Khalifa [3] mentioned that the reason for the use of iron waste in construction is because it is useful for both the economy and the environment; he concluded that there is an increase in industrial and technological by-products which are hazardous for both the environment and human health if not properly disposed of. Moreover, these by-products are the main cause of the evaporation of CO_2 and other harmful gases which cause global warming and the destruction of the ozone layer which protects the planet earth from harmful cosmic rays. Also, industrial wastes and by-products can be used as substitute materials in concrete and building units, which in itself is a better alternative to dumping such wastes as it will protect the environment and alleviate the consumption of natural resources.

Nadeem and Pofale [4] utilized granular slag as a replacement of natural fine aggregate in construction applications such as masonry and plastering. In this investigation, cement mortar mixes 1:3, 1:4, 1:5 and 1:6 by volume were selected for 0%, 25%, 50%, 75% and 100% replacements of natural sand with granular slag for w/c ratios of 0.60, 0.65, 0.70 and 0.72, respectively. The sand replacement from 50% to 75% improved mortar flow properties by 7%, whereas the compressive strength improved by 11–15% at the replacement level from 25% to 75%. At the same time brick mortar crushing and pull strengths improved by 10–13% at 50–75% replacement levels. The study concluded that, granular slag could be utilized as alternative construction material for natural sand in masonry and plastering applications either partially or fully. Ansu and Elson [5] studied the utilization of induction furnace slag as an alternative for conventional fine aggregate. In this study the compressive strength of mortar and concrete made with partial replacement of fine aggregate using induction furnace slag was determined. Pertaining to the experimental investigation, mixes were prepared with fine aggregates replacement using 20%, 30%, 40%, 50% and 60% induction furnace slag. Compressive strength tests on mortar and concrete were conducted and the obtained results indicated that fine aggregates replacement using 30% induction furnace showed a better performance compared to the control mix.

The main objective of this investigation is to study the effect of partial replacement of sand by the basic-oxygen furnace slag (BOFS) at percentages of 0%, 40%, 80% and 100% on the physico-mechanical properties of cement mortar and also study the attenuation of gamma-rays via heavy density mortar incorporating slag-fine aggregate using the radioisotopes of ^{137}Cs and ^{60}Co sources.

Experimental program

Materials

The material properties of mortar mix proportions and procedures for the preparation of mixes are discussed in this section. Type I Portland cement-CEM I (42.5 N), provided from Suez Cement Company in compliance with the requirements of ASTM C-150 [6] was used. Table 1 outlines the chemical composition using XRF Spectrometer PW 1400 and physical characteristics of the cement. The natural aggregate used for the preparation of cement mortar was sand (S). The basic-oxygen furnace slag (BOFS) with high density was used as a partial replacement material for natural aggregate, which is extensively produced as a by-product through iron and steel production at the Egyptian Iron and Steel Company, Helwan, Egypt.

Both sand and crushed slag were washed with water to remove the contaminated fine materials and oven dried at 100 °C for 24 h. The aggregates were passed through a sieve of 1 mm and retained on a sieve of 600 μm. The chemical composition and physical properties of fine aggregates are presented in Table 2. The main chemical constituents of the basic-oxygen furnace slag are CaO, Fe_2O_3 and SiO_2. During the conversion of molten iron into steel, a percentage of the iron (Fe) in the hot metal cannot be recovered into the steel produced. This oxidized iron is observed in the chemical composition of the BOF slag [7]. The results in Table 2 indicate that, oxygenated slag has higher specific gravity and volumetric weight than natural sand whereas the percentage of clay

Table 1 Chemical composition and physical characteristics of cement (OPC-CEM I).

Oxides (mass, %)		Physical characteristics	
SiO_2	21.26	Specific gravity	3.15
Al_2O_3	4.49	Consistency	24%
Fe_2O_3	3.49	Blaine's specific surface (cm^2/kg)	2415
CaO	63.81	Initial setting time	103 min
MgO	2.02	Final setting time	211 min
SO_3^{--}	3.11		
Cl^-	0.03		
Na_2O	0.14		
K_2O	0.09		
TiO_2	–		
BaO	–		
P_2O_5	–		
L.O.I	1.57		
Total	99.98		

Please cite this article in press as: A.S. Ouda, H.A. Abdel-Gawwad, The effect of replacing sand by iron slag on physical, mechanical and radiological properties of cement mortar, HBRC Journal (2015), http://dx.doi.org/10.1016/j.hbrcj.2015.06.005

Table 2 Chemical composition and physical properties of fine aggregates.

Oxides	BOFS	S	Physical characteristics	BOFS	S	Limits for fine aggregates
SiO_2	8.20	94.84	Specific gravity	2.71	2.5	–
Al_2O_3	0.73	2.12	Volumetric weight (t/m^3)	1.87	1.74	–
Fe_2O_3	38.89	0.82	Clay and fine materials (%)	19.6	1.8	⩽4[a]
CaO	39.52	0.52				
MgO	0.88	0.1				
SO_3^{--}	0.24	0.11				
Cl^-	–	0.06				
Na_2O	–	0.27				
K_2O	–	0.69				
TiO_2	0.22	0.12				
BaO	0.13	–				
P_2O_5	2.20	0.04				
L.O.I	0.11	0.22				
Total	99.96	99.91				

[a] According to ESS 1109 [8].

and fine materials in slag were several times higher than that of natural sand.

Preparation of mortar mixes

Four mixes were prepared by replacing natural sand with 0%, 40%, 80% and 100% basic-oxygen furnace slag by mass. The mix proportions of the studied mortars are listed in Table 3. The water-to-cement ratio (w/c) was 0.44 by mass. The ratio of cement: aggregate was 1:3 for the four mixes at dry condition. Dry mixtures were placed in a standard 5 l capacity bench-mounted mixer to ensure complete homogeneity, after that the required amount of mixing water was poured to the dry mix. Continuous and vigorous mixing was conducted for 5 min. Each specimen was then cast into $25 \times 25 \times 25$ mm cubic steel molds, and manually pressed into the corners and along the surface of the mold until a homogeneous paste was obtained. After the top layer was compacted and pressed with hand, the surface of the paste was smoothed by the aid of thin edged trowel. The specimens were left at 100% relative humidity for 24 h. After demolding, specimens were cured in a water tank for 90 days.

Testing method and procedure

The compressive strength of the prepared mortars was measured according to the ASTM specification [9] using five tones German Brüf pressing machine with a loading rate of 100 kg/min. At each time of curing, the crushed samples were subjected to stopping of hydration by using a mixture of acetone and methanol in the ratio of 1:1 by volume, followed by drying to 80 °C for 24 h to prevent further hydration, after that the dried samples were kept in a desiccators for further analysis [10]. The bulk density of the cement mortars was measured up to 90 days in accordance with [11].

The attenuation measurements of gamma rays were performed using sodium iodide NaI (Tl) scintillation detector with a Multi Channel Analyzer (MCA). The schematic diagram of the experimental setup is shown in Fig. 1. The utilized radiation sources comprised ^{137}Cs and ^{60}Co radioactive elements with photon energies of 0.662 MeV for ^{137}Cs and two energy levels of 1.173 and 1.333 MeV for ^{60}Co as standard sources with activities in micro curie (5 mCi). Tests were carried out on cylindrical specimens of large dimensions, 10 cm diameter. Each specimen was cut by saw to slices of different thickness, ranging from 20 to 80 mm. After 28 days of water curing, specimens were taken out and left to oven dry at 105 °C prior conducting the test as recommended by Yilmaz et al. [12]. The tested samples with different thicknesses were arranged in front of a collimated beam emerged from gamma ray sources. The measurements were conducted for 20 min counting time for each sample. The attenuation coefficient of gamma rays was determined by measuring the fractional radiation intensity N_x passing through the thickness x as compared to the source intensity N_o. The linear attenuation coefficient (μ) has been obtained from the solution of the exponential Beer–Lambert's law [13].

$$N_x = N_o^{e-\mu x}\ \mathrm{cm}^{-1} \quad (1)$$

Table 3 Proportions of aggregate percentages in mortar mixtures, (1:3).

Mixture labels	Mortar mix proportions (%)			
	OPC	S	BOFS	w/c ratio
M1	25	75	–	0.44
M2	25	45	30	0.44
M3	25	15	60	0.44
M4	25	–	75	0.44

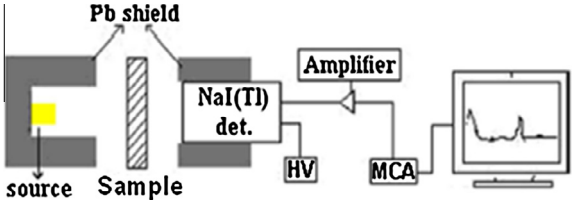

Fig. 1 Schematic diagram for test arrangement.

The total mass attenuation coefficients, μ_m, are also given as follows:

$$\mu_m = \mu/\rho = (1/\rho \cdot x)\ln(N_o/N)\ \mathrm{cm}^2/\mathrm{g} \quad (2)$$

where ρ is the density of sample.

The effectiveness of γ-ray shielding is described in terms of the half-value layer (HVL) or the tenth-value layer (TVL) of a material. The HVL is the thicknesses of an absorber that will reduce the γ-radiation to half and the TVL is the thicknesses of an absorber that will reduce the γ-radiation to one tenth of its original intensity. Those are obtained using the following equations [14]:

$$\mathrm{HVL} = \mathrm{In}\,2/\mu \quad (3)$$

$$\mathrm{TVL} = \mathrm{In}\,10/\mu \quad (4)$$

The mean free path (mfp) is defined as the average distance between two successive interactions of photons and it is given as:

$$\mathrm{mfp} = 1/\mu \quad (5)$$

Results and discussion

Compressive strength of hardened mortar

The variation in the compressive strength of cement mortars incorporating different proportions of oxygen-furnace slag as a replacement for sand after curing in water for 90 days is graphically represented in Fig. 2. In general, all mortar mixes exhibited progressive increase in compressive strength with increasing curing time up to 90 days, as a result of the filling up of the open pores with hydration products caused by cement hydration to form a denser and a closer mortar structure. Evidently, the compressive strength increased by about 22%, 10%, 15%, 23% and 21% for 40% replacement level of slag (M2) at curing ages of 1, 3, 7, 28 and 90 days, respectively, compared to the control mix (M1), while the increase in compressive strength was 26%, 19%, 27%, 32% and 30% upon replacing sand by 80% slag (M3). On the other hand, mortar mix M4 (containing 100% BOFS) exhibited the highest compressive strength among all blends, as it has achieved 32%, 31%, 39%, 40% and 38% higher compressive strength values compared to the control mix. The increase in the compressive strength could be attributed to the adhesion between crystallized slag aggregate and cement paste due to rough surface of slag aggregate which ensured strong bonding between aggregate particles and cement paste [4]. The aforementioned results showed that the optimum percentage of BOFS replacement is 100%, which has a noticeable effect on the compressive strength of mortar, therefore, steel slag can be used to fully replace sand in the cement mortar.

Bulk density of hardened mortar

Fig. 3 presents the bulk density of cement mortars made of steel slag at percentages of 0%, 40%, 80% and 100% as a replacement for sand, submerged in water for 90 days. It was noted that, a marginal increase in the bulk density for all mixes was observed with increasing curing time up to 90 days. Mortar containing 40% of BOFS (M2) showed a steady increase in bulk density of about 7% for all curing ages as compared to the control mix (M1). As the basic-slag replacement increases, the cement mortar containing 80% (M3) demonstrated higher values of the bulk density than that incorporating sand by approximately 18% for testing ages of 1, 3, 7, 28 and 90 days. On the other side, the bulk density was significantly increased by about 23% for all testing ages at full sand replacement (M4) compared to the control mix. This possibly can be attributed to the increase in the specific gravity of oxygen slag aggregate in comparison with sand (Table 2); in addition to micro-pores on the surface of crushed aggregate which can be filled with cement paste which in turn increases the interlocking bond between aggregate particles and the cement matrix, therefore, the total porosity decreases and the bulk density increases.

Gamma-ray attenuation properties

Photon attenuation coefficient is an important parameter for characterizing the penetration and diffusion of γ-rays in the multi-element materials. The scattering and absorption of

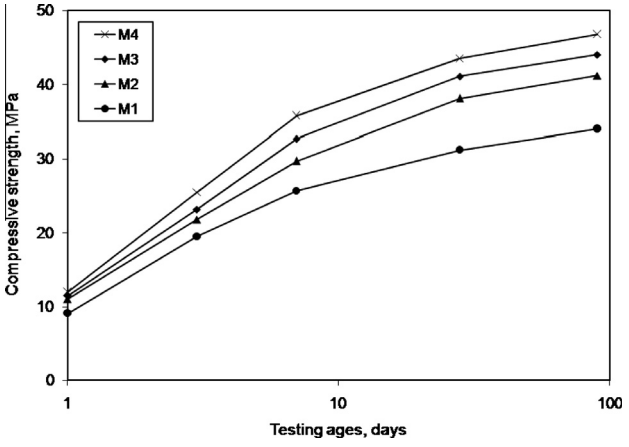

Fig. 2 Compressive strength of cement mortars due to replacing sand by the basic-oxygen furnace slag (BOFS) at percentages of 0%, 40%, 80% and 100%, submerged in water for 90 days.

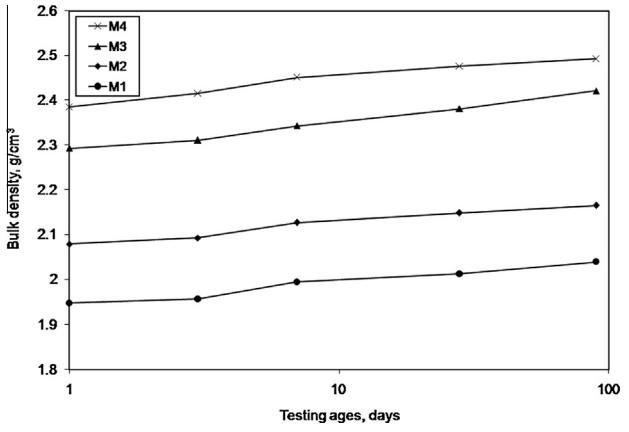

Fig. 3 Bulk density of cement mortars due to replacing sand by the basic-oxygen furnace slag (BOFS) at percentages of 0%, 40%, 80% and 100%, submerged in water for 90 days.

Table 4 The measured values of μ, μ_m, HVL, TVL and mfp for mixes M1 and M4 at photon energies of 0.662 MeV for ^{137}Cs and two photon energies of 1.173 and 1.333 MeV for ^{60}Co sources.

Mixes	Radioisotope	Thickness (mm)	ρ (ton/m^3)	μ (cm^{-1})	μ_m (cm^2 g^{-1})	HVL (cm)	TVL (cm)	mfp (cm)
M1	^{137}Cs	20	2.017	0.1534	0.07605	4.517	15.009	6.519
		40	2.209	0.1537	0.06957	4.508	14.980	6.506
		60	2.240	0.1552	0.06928	4.465	14.835	6.443
		80	2.252	0.1621	0.07198	4.275	14.204	6.169
M1	^{60}Co	20	2.017	0.1490	0.07387	4.651	15.453	6.711
		40	2.209	0.1492	0.06757	4.642	15.425	6.699
		60	2.240	0.1507	0.06729	4.597	15.273	6.633
		80	2.252	0.1574	0.06989	4.402	14.628	6.353
M4	^{137}Cs	20	2.481	0.1887	0.07605	3.672	12.202	5.299
		40	2.521	0.1917	0.07602	3.615	12.010	5.216
		60	2.601	0.1933	0.07862	3.585	11.911	5.173
		80	2.631	0.2001	0.07604	3.463	11.506	4.997
M4	^{60}Co	20	2.481	0.1832	0.07386	3.781	12.564	5.456
		40	2.521	0.1862	0.07384	3.721	12.364	5.369
		60	2.601	0.1876	0.07634	3.692	12.267	5.327
		80	2.631	0.1943	0.07386	3.565	11.847	5.145

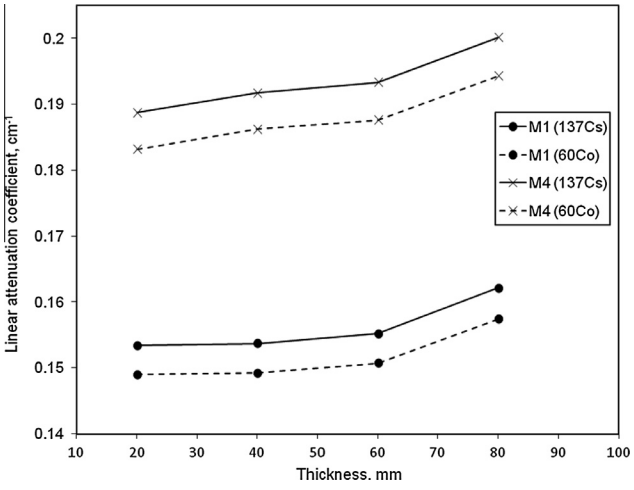

Fig. 4 Linear attenuation coefficients as a function of shield thicknesses for mortar mixes at photon energies of 0.662 MeV for ^{137}Cs and two photon energies of 1.173 and 1.333 MeV for ^{60}Co sources.

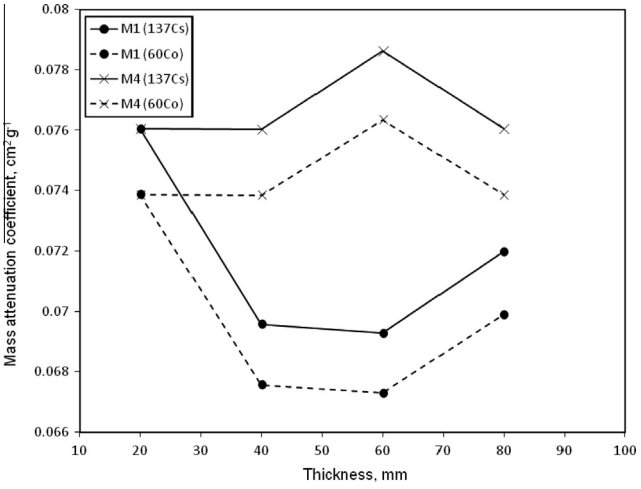

Fig. 5 Mass attenuation coefficients as a function of shield thicknesses for mortar mixes at photon energies of 0.662 MeV for ^{137}Cs and two photon energies of 1.173 and 1.333 MeV for ^{60}Co sources.

gamma radiations are related to density and effective atomic numbers of material, consequently, knowledge of the mass attenuation coefficients is of prime importance. However, the linear (μ, cm^{-1}) or mass attenuation [μ_m (cm^2 g^{-1})] coefficients, which are defined as the probability of all possible interactions between γ-rays and atomic nuclei, have been mentioned to investigate the radiation shielding properties of any shielding materials. These attenuation coefficients depend on the incident photon energy and the chemical composition of the absorbing material's parameters such as their types, thickness and densities [15]. The values of linear and mass attenuation coefficients for cement mortars incorporating sand and basic-oxygen furnace slag aggregates have been measured by a scintillation detector (Fig. 1) at photon energy of 0.662 MeV for ^{137}Cs and two photon energies of 1.173 and 1.333 MeV for ^{60}Co. The thickness and density of each sample which is necessary in order to derive the linear and mass attenuation coefficients from the measured incident and transmitted gamma-ray intensities are shown in Table 4.

The measured linear and mass attenuation coefficients as a function of different shield sample thickness for mixes M1 and M4 have been displayed in Figs. 4 and 5. It can be seen that, linear attenuation coefficients of specimens M1 and M4 increase up slightly with thicknesses, while, those values go down linearly with increasing the photon energies obtained from ^{137}Cs and ^{60}Co sources (Fig. 4). It means that the increase of photon energy from 0.662 MeV for ^{137}Cs up to 1.333 MeV for ^{60}Co decreases the attenuation rate for mixes in the field of γ-rays. On the contrary, the values of mass attenuation coefficient decrease with thicknesses of M1 and M4 mixes as

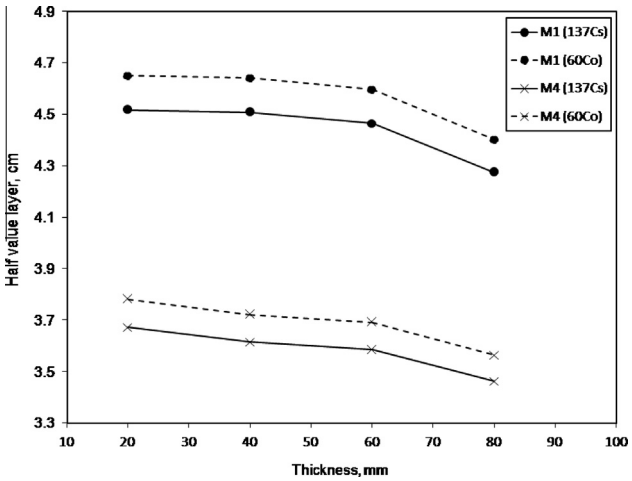

Fig. 6 Half value layer of mortar mixes at photon energies of 0.662 MeV for ^{137}Cs and two photon energies of 1.173 and 1.333 MeV for ^{60}Co sources.

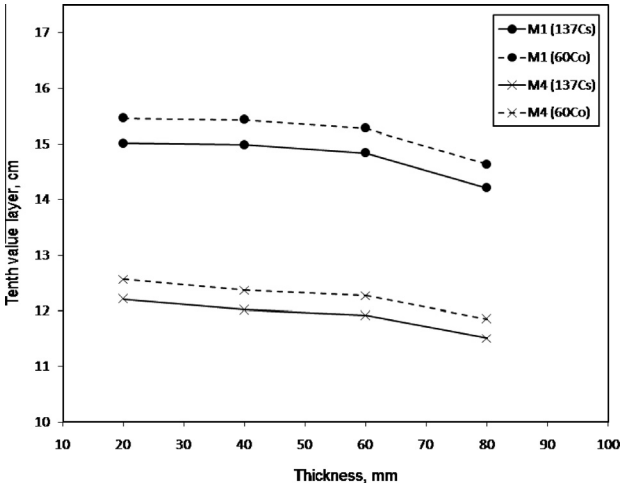

Fig. 7 Tenth value layer of mortar mixes at photon energies of 0.662 MeV for ^{137}Cs and two photon energies of 1.173 and 1.333 MeV for ^{60}Co sources.

indicated in (Fig. 5). Additionally, the values of μ_m irregularly decrease with photon energies (0.662 MeV $\leqslant$ Eg. $\leqslant$ 1.333 MeV) for M1 and M4, which indicates the different photon absorption mechanism for different photon energies [16]. With regard to gamma-ray shielding, the percentage of slag in mortar increases the density of the sample, because the mixes with slag have high iron content. Evidently, mix M4 (incorporating slag aggregate) attenuates more gamma radiation at photon energies irradiated by ^{137}Cs and ^{60}Co sources. Mix (M4) has a higher density compared to mix (M1) (control mix), therefore, it is considered the best for shielding purposes in this research as it provided the highest attenuation values. This trend is mainly attributed to the high specific gravity of the slag aggregate (Table 2).

The values of half-value layer (HVL) and tenth value layer (TVL) of mixes M1 and M4 at different doses of gamma irradiation emitted by ^{137}Cs and ^{60}Co are graphically plotted as a function of shield thickness in Figs. 6 and 7. As is evident from

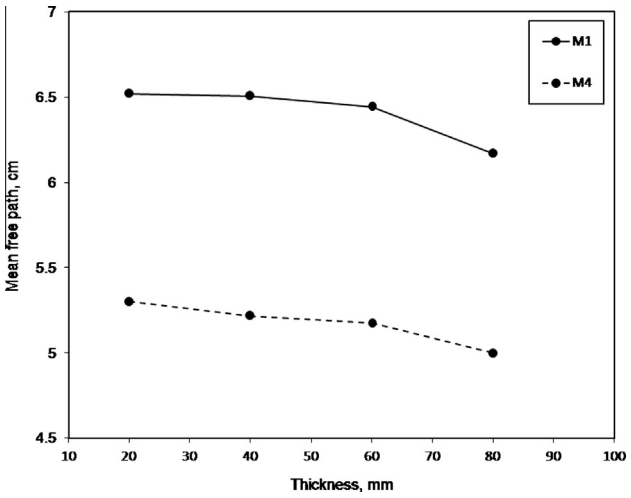

Fig. 8 The variation of mean free path as a function of the mortar thickness at photon energy of 0.662 MeV for ^{137}Cs source.

the figures, the values of HVL and TVL decrease with the increase of attenuation thicknesses in the field of gamma radiation at different photon energies. At lower gamma ray energy of 0.662 MeV, the values of HVL and TVL are lower for mix M4 in comparison with mix M1 at the same dose. The results also revealed that, the values of half and tenth layers increase with high-energy photon dose, accordingly, the HVL and TVL for mixes M1 and M4 irradiated by ^{60}Co at two photon energies of 1.173 and 1.333 MeV are higher than those exposed to dose of 0.662 MeV emitted by ^{137}Cs source. As set out in Table 4, the HVL and TVL values are inversely proportional with the density, for that, mix M4 with high density showed lower values of HVL and TVL than that of mix M1 at different photon energies and consequently, mix M4 is remarkably effective for shielding gamma rays.

The mean free path (mfp) represents the average distance between two successive photo interactions. The shorter mfp indicates more interaction of photons to material and hence possesses the better shielding properties [16], and that it is the reciprocal of the measured linear attenuation coefficients. In this investigation, the variation of mean free path (mfp) as a function of the samples thickness for the two mixes M1 (control mix) and M4 (incorporating 100% slag) was measured at different photon energies of 0.662, 1.173 and 1.333 MeV. The results are displayed in Figs. 8 and 9 for ^{137}Cs and ^{60}Co sources, respectively. These figures indicate that the mean free path increases with the increase of high-energy photon doses; accordingly, sample M1 exhibited the highest mfp values at two photon energies of 1.173 and 1.333 MeV for ^{60}Co, i.e., lower attenuation coefficient values at similar loading rates of the radiation source as compared to M4. This may be attributed to the low specific gravity of sand in mortar as opposed to that of slag (Table 2). It is common that increasing the relatively heavy aggregate contents within cement mortar improves its bulk density.

The density of the anti radiation shielding material is an important factor in attenuation. Hence reduction of porosity levels and incorporating particulates of high specific gravity enhance the attenuation performance of the matrix. The results also indicated that the measured mfp is inversely proportional

Please cite this article in press as: A.S. Ouda, H.A. Abdel-Gawwad, The effect of replacing sand by iron slag on physical, mechanical and radiological properties of cement mortar, HBRC Journal (2015), http://dx.doi.org/10.1016/j.hbrcj.2015.06.005

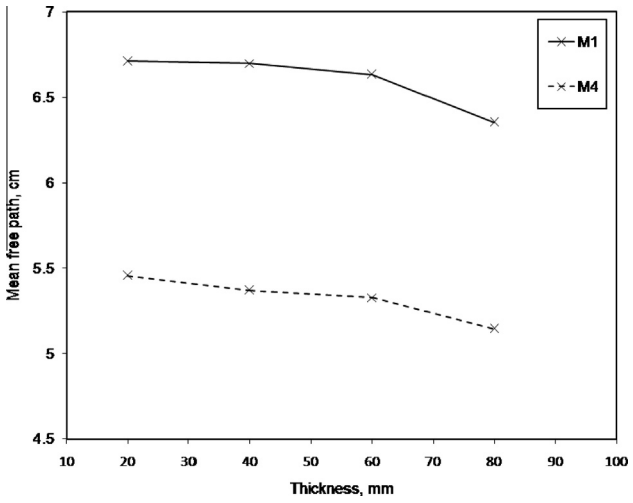

Fig. 9 The variation of mean free path as a function of the mortar thickness at two photon energies of 1.173 and 1.333 MeV for ^{60}Co source.

to the density of cement mortar. The mix which contains 100% slag aggregate (M4) exhibited the lower values for mfp at different photon energies obtained from ^{137}Cs and ^{60}Co radioisotopes when compared to mix M1. This tendency is derived primarily from the high close packing of the aggregates which consequently lead to the reduction in porosity level and improvement in the bulk density; consequently, substantial improvement in attenuation performance at photon energies for ^{137}Cs and ^{60}Co gamma ray sources.

Conclusions

The following conclusions can be drawn based on the experimental findings and discussion of the study conducted:

1. The incorporation of the basic-oxygen furnace slag (BOFS) in cementitious mortars at 40%, 80% and 100% replacement improves the physico-mechanical characteristics for mixes than normal mortar made of sand.
2. Mortar sample of full sand replacement exhibited the highest compressive strength among all mixes, as it had 32%, 31%, 39%, 40% and 38% higher values compared to the control mix.
3. Heavy density mortar made of 100% slag as fine aggregate has significant effects on shielding efficiency in thin mortar shields (up to 8 cm) by using radiation sources comprised ^{137}Cs of 0.662 MeV and ^{60}Co with two energy levels of 1.173 and 1.333 MeV, because it reduces the captured gamma rays better than normal mortar.
4. Based on this study, it is concluded that percentage iron slag can fully replace sand in cement mortar.

Conflict of interest

The authors declare that they have no conflict of interest.

References

[1] R. Alizadeh, M. Chini, P. Ghods, M. Hoseini, Sh. Montazer, M. Shekarchi, Utilization of electric arc furnace slag as aggregates in concrete, in: 6th CANMET/ACI International Conference on Recent Advances in Concrete Technology Bucharest Romania, 2003, pp. 451–464.
[2] W. Gutt, P.J. Nixon, M.A. Smith, W.H. Harrison, A.D. Russell, A Survey of the Locations Disposal and Prospective uses of the Major Industrial by-Products and Materials, U.K Build Res Establishment Watford, 1974.
[3] J. Khalifa, Using copper slag as a construction material, in: Proceedings of the International Conference of High Performance Construction Materials, Ostend Belgium, 2006.
[4] M. Nadeem, A.D. Pofale, Replacement of natural fine aggregate with granular slag – a waste industrial by-product in cement mortar applications as an alternative construction material, Int. J. Eng. Res. Appl. 21 (2012) 1258–1264.
[5] J. Ansu, J. Elson, Study on the partial replacement of fine aggregate using induction furnace slag, Am. J. Eng. Res. 4 (2013) 1–5.
[6] ASTM C150. Standard Specification for Portland Cement, 2009.
[7] I.Z. Yildirim, M. Prezzi, Chemical, mineralogical and morphological properties of steel slag, Adv. Civ. Eng. (2011) 1–13.
[8] Egyptian Standard Specifications No. 1109. Concrete Aggregates from Natural Sources, 2002.
[9] ASTM C109. Standard Test Method for Compressive Strength of Hydraulic Cement Mortars, 2007.
[10] A.S. Taha, H. El-Didamony, S,A. Abo EL-enein, H.A. Amer, Physicochemical properties of supersulphated cement pastes, Zement Kalk Gips 34 (1981) 351–353.
[11] L.E. Copeland, T.C. Hayes, Porosity of hardened Portland cement pastes, J. Am. Concr. Inst. 27 (1956) 633–640.
[12] E. Yilmaz, H. Baltas, E. Kiris, I. Ustabas, U. Cevik, A.M. El-khayatt, Gamma ray and neutron shielding properties of some concrete materials, Ann. Nucl. Energy 38 (2011) 2204–2212.
[13] M.H. Kharita, S. Yousef, M. Al- Nassar, Review on the addition of boron compounds to radiation shielding concrete, Prog. Nucl. Energy 53 (2011) 207–211.
[14] K. Singh, H. Singh, V. Sharma, R. Nathuram, A. Khanna, R. Kumar, S.S. Bhatti, H.S. Sahota, Gamma-ray attenuation coefficients in bismuth borate glasses, Nucl. Instrum. Meth. B 194 (2002) 1–6.
[15] I. Akkurt, B. Mavi, A. Akkurt, C. Basyigit, S. Kilincarslan, H.A. Yalim, Study on Z-dependence of partial and total mass attenuation coefficients, J. Quant. Spectrosc. Radiat. Transfer 94 (3–4) (2005) 379–385.
[16] N. Chanthima, J. Kaewkhao, Investigation on radiation shielding parameters of bismuth borosilicate glass from 1 keV to 100 GeV, Ann. Nucl. Energy 55 (2013) 23–28.